Crystal Growth

Emergence of Morphological Chirality from Twinned Crystals**

Hiroaki Imai and Yuya Oaki*

Helical and spiral architectures are fundamental shapes that have chirality and are observed in various environments and scales in nature. Their unique morphology is fascinating; the formation mechanisms for many kinds of helical forms are still a mystery. Biological polymers such as DNA, collagen, and agar produce helical chains from the nanometer to the submicron scale with a specific interaction through hydrogen bonding.[1] Artificially produced chiral organic molecules,[2] polymer chains,[3,4] and macromolecules[5] have been reported to induce twisted aggregates on various scales. In general, the formation of these helices was ascribed to the chirality of the components and hydrogen bonding originating from their asymmetric molecular structure. However, helical morphologies are not always attributable to only microscopic chirality at a molecular level. For example, macroscopic helical morphologies have also been observed with organic molecules,[6] polymers[7] and inorganic materials [8,9,13–18] without microscopic chirality. Helical whiskers, produced by vapor-phase deposition techniques, originate from the asymmetric behavior of a growing site at the top of each whisker[8] and dislocations in the crystal phase.[9] Well-known twisted ribbons in spherulites of polymer crystals without chirality have been characterized by X-ray diffraction and by modeling.[10,11] It was reported in 1929 that that several organic and inorganic crystal systems, except for cubic systems, induce twisted shapes.[12] However, the details of the shapes and growth conditions have not been previously described in the literature. In recent years, new families of helical shapes were discovered for barium sulfate,[13] calcium,[14] barium and strontium carbonates,[15] potassium dichromate,[16] manganese oxide,[17] and silica–surfactant composite.[18] Consequently, a novel concept is required to understand the emergence of these morphological chirality from achiral components.

We found that helical morphologies are generally grown with triclinic crystals in various kinds of gel matrices. The backbone of the unique architectures was observed to be

[*] Prof. H. Imai, Y. Oaki
Department of Applied Chemistry
Faculty of Science and Technology
Keio University
3-14-1 Hiyoshi, Kohoku-ku, Yokohama 223-8522 (Japan)
Fax: (+81) 45-566-1551
E-mail: hiroaki@applc.keio.ac.jp

[**] This work was supported by Grant-in-Aid for Scientific Research (No. 15560587) and 21 st Century COE program "KEIO Life Conjugate Chemistry" from the Ministry of Education, Culture, Sports, Science, and Technology, Japan. We thank Prof. D. K. Kondepdi at Wake Forest University for critically reading the manuscript.

Supporting information for this article is available on the WWW under http://www.angewandte.org or from the author.

 DOI: 10.1002/ange.200352891

composed of twin crystals twisted with a constant angle. The emergence of the macroscopic chiral morphology from achiral components is attributable to twisted assembly of tilted units in a diffusion field. Moreover, right-handed helices were predominantly obtained in a gel matrix consisting of biological macromolecules.

In total, four kinds of inorganic materials, including triclinic crystals ($K_2Cr_2O_7$ and H_3BO_3) and the cubic crystals ($Ba(NO_3)_2$ and NH_4Cl), were grown in various sorts of organic gel media (poly(vinyl alcohol) (PVA), poly(acrylic acid) (PAA), gelatin, agar, and pectin,). Crystals were grown from the precursor that contained a specified amount of the inorganic materials and gelling agents by lowering the temperature[19] (method 1) or by evaporation of water from the precursor (method 2). Detailed experimental procedure and conditions are described in the Experimental Section and in the figure legends.

As we have already reported,[19] the morphology of crystals grown in gel media by lowering the temperature (method 1) varied with the gel density. The fundamental variation of the morphologies was independent of the sorts of grown crystals and gelling agents. Polyhedral forms changed into skeletal and then dendritic shapes with increasing gel density. This evolution is ascribed to the change of growth behavior from a kinetic-limited mode into a diffusion-limited mode with suppression of the mobility of the solutes in the presence of gelling agents.[19] The main role of the gelling agents was the suppression of diffusion and the formation of a diffusion field. Consequently, gel media control the diffusion process and are otherwise inert for crystal growth. As shown in Figure 1 a–d, connected crystals consisting of platy subunits were produced through diffusion-limited growth with increasing gel density (method 1). Finally, twisted morphologies were observed in the branches of dendritic and spherulitic forms of the triclinic crystals ($K_2Cr_2O_7$ and H_3BO_3) grown in gel media at a relatively high density, regardless of the gelling agent. We could not detect the influence of the gelling agents on the crystallization process as a source of nucleation sites or scaffolds. Helical morphology also formed in the same growth condition by method 2 (Figure 1 e,f). On the other hand, twisted shapes were never found with cubic crystals (($Ba(NO_3)_2$, NH_4Cl)) under any conditions. These results suggest that the helical aggregates were produced through a diffusion-limited growth of triclinic crystals. However, detailed information of the structure of the unique aggregates was not obtained from the results shown in Figure 1.

We have successfully revealed the backbone for the foundation of helical aggregates, as shown in Figure 2 a–d. The twisted backbone was composed of platy subunits with a rotated connection both for $K_2Cr_2O_7$ and H_3BO_3, even though the shapes of the subunits are different. When the twisted platy subunits were not directly recognized on several helical forms as shown in Figure 1 f, the magnified SEM and TEM images clearly indicated the presence of the backbone inside the aggregates (Figure 3). Since the angles between the platy subunits at the connections were constant (Figure 2 c,d), the twisted backbone is deduced to be composed of twinned crystals. Tilted parallelogram subunits of $K_2Cr_2O_7$ surrounded by the $(2\bar{1}1)$, (010), and (001) planes were aligned along the

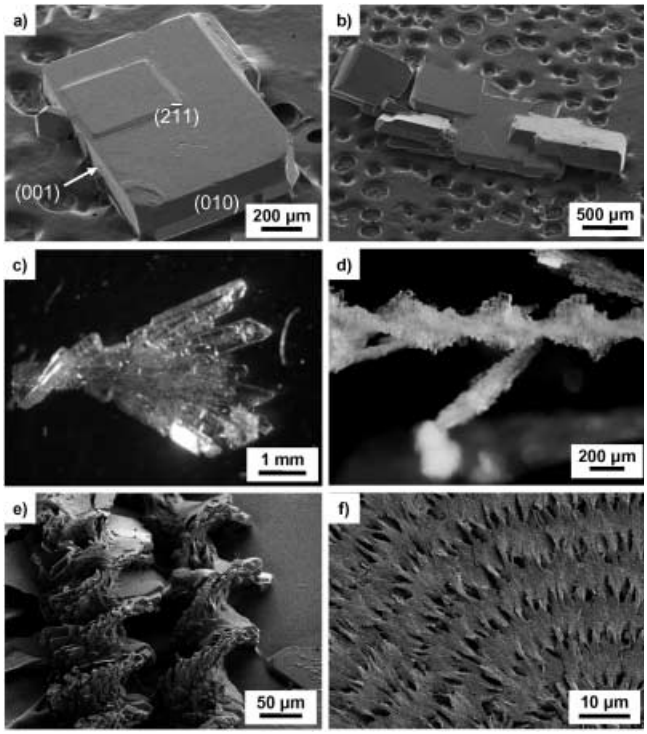

Figure 1. Typical optical microscopy and field-emission scanning electon microscope (FESEM) images of the twisted and helical architectures. a) Platy crystals at $C_{KC}=25.0$, $C_{ge}=0$, b) connection of the platy subunit crystals at $C_{KC}=25.0$, $C_{ge}=5.0$, c) twisted morphology consisting of the connections at $C_{KC}=25.0$, $C_{ge}=20.0$, d) helical forms at $C_{KC}=25.0$, $C_{ge}=25.0$. Twisted and helical morphology was formed through the connections of the platy subunits crystals with an increase of gel density (method 1; see Experimental Section). Various helical morphology grown by method 2 at $C_{KC}=3.0$, $C_{pe}=0.3$ (e), and $C_{KC}=2.0$, $C_{PAA}=0.02$ (f). These unique morphologies were found on triclinic crystals through diffusion-limited growth in gel matrices.

b axis with a rotation angle of about 12°. Hexagonal plates composed of the (100), (010), (001), and $(\bar{1}10)$ planes of H_3BO_3 were strung along the $\langle 100\rangle$, $\langle 010\rangle$, or $\langle \bar{1}10\rangle$ direction with a rotation angle of about 4.5°. The coincident lattice matching at the angles is estimated to be relatively good for these crystals because a suitable twin lattice with periodicity could be formed at the twin plane (see Supporting Information). Thus, the helical forms can be called "twisted twins." The rule of the connections was independent of the sorts of the gel matrices. The variation of the pitch of the helices depended on a change in the size of the subunits. A reduction in size increased the pitch of the twisting of the backbone. Figure 2 g,h shows a model of the twisted backbone with platy subunits (Figure 2 e,f) that were estimated from SEM images and unit-cell structures of $K_2Cr_2O_7$ and H_3BO_3 with specific angles for the connections. The backbones of the helical morphologies experimentally obtained are approximately reproduced by this simple simulation. These results support the idea that the twisted backbone consists of twins. The formation of twisted twins is ascribed to an increase in the influence of diffusion upon crystal growth in the gel media.

Figure 4 shows a nucleation point of helical (a) H_3BO_3 and (b) $K_2Cr_2O_7$ crystals grown in agar and PAA, respectively.

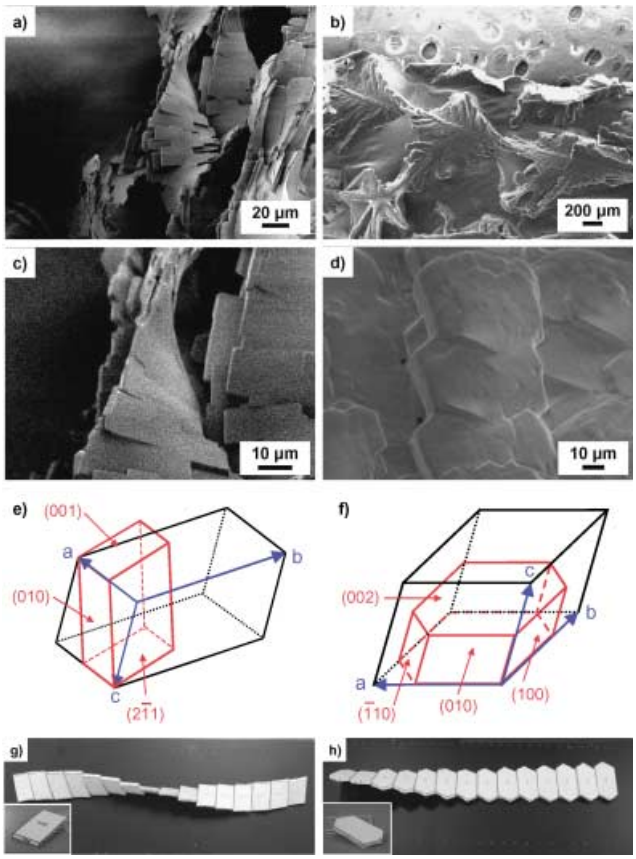

Figure 2. Backbone and detailed structure of unique helical forms. FESEM images of the backbone of (a) $K_2Cr_2O_7$ ($C_{KC}=3.0$, $C_{pe}=0.3$) and (b) H_3BO_3 ($C_{HB}=2.0$, $C_{ag}=0.2$) helices with twisted twins consisting of platy subunits. FESEM images of (c) $K_2Cr_2O_7$ and (d) H_3BO_3 twisted twins (magnification of (a) and (b), respectively). Schematic illustrations of (e) $K_2Cr_2O_7$ and (f) H_3BO_3 platy subunits estimated from FESEM images, XRD analysis, and unit cell structures. Simple models of the twisted backbones of (g) $K_2Cr_2O_7$ and (h) H_3BO_3 with platy subunits. We successfully obtained the backbone (a) and (b) of the helical morphologies consisting of the twisted twins (c) and (d). In addition, these morphologies were easily reproduced by a simple model (g) and (h) with platy subunits derived from those shown in (e) and (f).

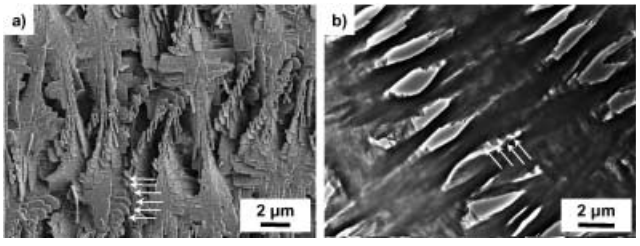

Figure 3. Magnified images of the backbone of the $K_2Cr_2O_7$ helical morphology. a) FESEM and b) TEM images clearly show the backbone structure of helical architecture consisting of the platy subunits.

Left- and right-handed twists are observed on the opposite side of the nucleation point. This observation suggests that the growth direction from the nucleation site determines the handedness of the helices. The specified direction of the twist did not change during the growth of the helical forms.

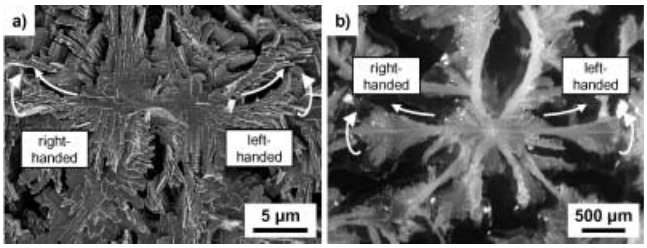

Figure 4. The nucleation point of (a) $K_2Cr_2O_7$ and (b) H_3BO_3 twisted forms grown in PAA and agar matrices, respectively. Left- and right-handed twists are observed on the opposite sides of the nucleation point, as indicated by the arrows.

Recently, Li, Cheng, and co-workers found the presence of twins in nanometer and micrometer scales in a helical polymer crystal consisting of chiral macromolecules.[20] Although their report also suggested the importance of twins for the construction of unique architectures, the correlation between the specific connections of twins and the helical morphology was not sufficiently clarified. The formation of helical architecture requires a pile of twisted twins with a constant angle and direction. Our results suggest that the architecture was achieved by the assembly of tilted subunits in a diffusion field. An increase in the gel density creates the condition for diffusion-limited growth by decreasing the mobility of solute molecules and ions. Consequently, the shapes of grown crystals change from polyhedral forms into regular dendrites and then into irregularly branching morphologies. The regular dendrites are usually composed of single crystals while the irregularly branching morphologies consisted of polycrystals. Thus, under highly diffusion-limited conditions, fast growth of the polycrystalline assembly is preferred over the formation of the more stable form of single crystals. In a diffusion field, the growth rate of a polycrystalline assembly is generally higher than that of single crystals because the growth along the direction of the highest gradient of the solute concentration is permitted in the former owing to an absence of a restriction of growth with specific crystal direction. Twin growth is inferred under moderately diffusion-limited conditions.[21,22] Therefore, the primary twisted unit is formed in a gel as twinned crystals (twins; Figure 1). Finally, the helical architecture is ascribed to assembly of the twinned crystals in a diffusion field. The connection is twisted owing to the tilt of the subunits originating from a lower symmetry of the triclinic crystal structure. The helical morphology with the triclinic crystals corresponds to the dendritic forms with cubic crystals.

When the diffusion process of solute molecules or ions determines the crystal growth, the gradient of the solute concentration around the growing surface is essential for the crystal morphology. The twisted assembly with a pile of tilted subunits in a diffusion field can be explained as follows: In a two-dimensional model, the higher driving force for crystal growth is obtained along direction A, which is the higher gradient of the concentration in a diffusion field (Figure 5a). The difference in the driving force is attributed to the asymmetry of a parallelogrammic subunit. In consequence, twins consisting of the same size of reverse subunits are

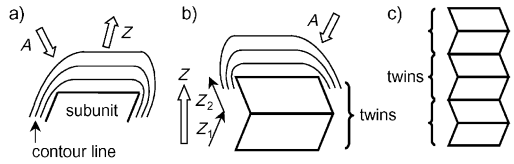

Figure 5. A two-dimensional growth model in a diffusion field. a) Growth of the asymmetric subunit along the higher concentration gradient (direction *A*) is preferable to the faster growth in a diffusion-limited condition. The gradient originated from the shape of the tilted subunit, b) thus, the reversed subunit forms the twins, and then the original growth direction (Z_1 and Z_2) is adjusted to *Z*. c) In this way, the faster growth was achieved to repeat formation of the twins.

produced to achieve faster growth as shown in Figure 5b, and the original growth direction (Z_1 and Z_2) is adjusted to direction *Z*. Since the more elongated reverse subunit would disturb the diffusion field and the faster growth, growth with the formation of the same size of the reverse twins is favorable even though excess interfacial energy is introduced. Therefore, a zigzag architecture would be created by the repetition of the twin formation (Figure 5c). Schultz also indicates that growth velocity is increased by spontaneous twin formation in twisted polymer crystals from the melt although experimental demonstration has not been carried out.[11] In three dimensions, the growth unit of triclinic crystals is tilted (Figure 6a). On the basis of the two-dimensional model, a pile of the same size of reverse subunits that rotate with an angle of 180° would be formed to achieve faster growth (Figure 6b). However, the nucleation probability of the completely reverse form is relatively small. Therefore, the growth direction *Z* is gradually adjusted by the accumulation of twins composed of slightly rotated subunits that have the same size as shown by Z_1, Z_2, Z_3... to Z_{15} (Figure 6). Since the angle of rotation is determined by the lattice matching on the twin plane, a series of twisted twins to reverse the growth direction is formed by a specified number of subunits with a constant angle. Then, the repetition of the twisted unit produces a continuous helical form (Figure 6g).

The direction of the rotation, which is associated with the handedness of the helices, depends on the tilt angle of the growth subunit. As shown in Figure 5b and Figure 6b, the growth direction *Z* of the tilted unit tends to be reversed in a diffusion field. In three dimensions, the daughter subunit is rotated to adjust *Z* toward the reversed position (Figure 6c). The rotated direction, clockwise or counterclockwise, could be explained as follows: Based on the assumption that the rotation of the daughter subunit around point O′ (the center of the top face of the mother subunit), movement of the furthest point P of the daughter subunit from point O (the center of the basal plane of the mother subunit) is essential to determine the rotation direction. Because the O–P distance provides the lowest concentration gradient for the growth of the tilted daughter subunit, the rotation with decrease in the O–P distance leads to advantageous growth conditions. The point P simply approaches the reverse position with counterclockwise rotation of the daughter subunit in the plan view of Figure 6c,d. In contrast, the O–P distance initially increases and then decreases with a clockwise rotation (Figure 6d). Since an increase in the O–P distance is disadvantageous for the reverse of the growth direction, counterclockwise rotation

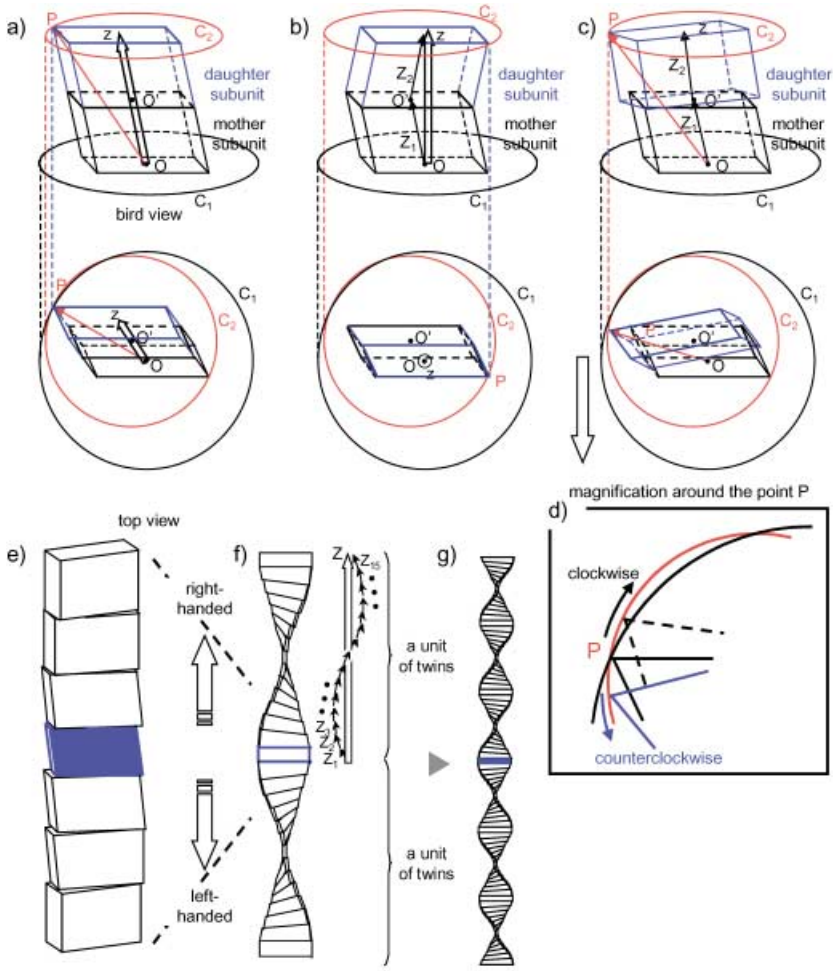

Figure 6. A three-dimensional growth model and formation mechanism of the helical morphology in a diffusion field. a) The growth subunit is tilted. b) The reverse twin could be formed to achieve the faster growth as seen in the two-dimensional model. c) In three dimensions, the formation of slightly rotated twin nuclei is more probable than that of reversed nuclei. d) Magnification of the region around point P, the twisted direction is determined by the variation of the O–P distance. In this case, counterclockwise rotation viewed from the upper sides is preferable to the clockwise rotation. e) According to this model, the upward and downward accumulations induce the right- and left-handed twists, respectively. f) Right- and left-handed units of twins are produced from the nucleation point. The growth direction (Z_1, Z_2, Z_3 to Z_{15}) is finally adjusted to *Z*. g) A pile of units forms helices; the specified direction of twist does not change during growth.

is more favorable than clockwise rotation. Repetition of the rotation with a certain direction produces a series of twisted twins. Eventually, the formation of daughter subunits on the mother subunit occurs with the counterclockwise rotation, and a right-handed helix is then created with the upward accumulation of subunits, as shown in Figure 6e–g. The counterclockwise rotation is also favorable when the daughter subunits grow under the mother subunit in a manner similar to that described in the previous discussion. In this case, however, a left-handed helix is produced with the downward growth, as shown in Figure 5f. Therefore, right- and left-handed helices would be equally generated with the upward and downward growth, respectively. Actually, right-handed helices were observed on the opposite side of left-handed helices as shown in Figure 4. The pair formation of left- and right-handed helices from a nucleation site strongly supports our model for the formation of helical morphologies. Helical morphologies consisting of H_3BO_3 are also attributable to the same formation mechanism, although the shape of the subunits is different. Interestingly, right-handed helices dominante in the media consisting of biological macromolecules such as agar, gelatin, and pectin, whereas almost the same amounts of left- and right-handed helices were observed in PAA and PVA matrices. This fact indicates that the macroscopic chiral symmetry breaking was induced by the homochirality of the biological molecules. This unique phenomenon could be explained by the twisted-twin model and the stereospecific interaction between the chiral molecules and crystal planes. Details of the specific interaction on the surfaces of triclinic crystals are now under investigation. We identified the backbone of helical morphologies consisting of triclinic crystals. The essence of the formation of the chiral architecture from achiral components is the rotated accumulation of tilted subunits under conditions of diffusion-limited growth. The triclinic crystal structure is not always required for the formation of tilted-growth subunits. Thus, the formation model proposed here would be applicable to various helical architectures and complex morphologies, including twisted ribbons in polymer spherulites. The results described herein provide a novel guideline to the morphogenesis of various helical and twisted forms.

Experimental Section

Materials: We produced two kinds of triclinic crystals, potassium dichromate ($K_2Cr_2O_7$; Kanto chemical, 99.5%) and boric acid (H_3BO_3; Kanto chemical, 99.5%), in gel media to obtain conditions conducive to diffusion-limited growth. These products easily crystallized in aqueous solutions because their solubility varied steeply with temperature. Crystal growth occurred in supersaturated solutions in a gelling agent, such as PVA ($\bar{M}_w = 22000$; Junsei chemical), poly (acrylic acid) ($\bar{M}_w = 250000$, 35wt% aqueous solution; Aldrich chemical), gelatin (Kanto chemical), agar (Junsei chemical), and pectin (Kanto Chemical). Cubic crystals, barium nitrate ($Ba(NO_3)_2$; Koso chemical, 99.0%) and ammonium chloride (NH_4Cl; Kanto chemical, 99.0%), were also prepared by using the same conditions as a contrastive experiment.

Crystallization method 1**:** Inorganic crystals ($K_2Cr_2O_7$, H_3BO_3, $Ba(NO_3)_2$, NH_4Cl) were dissolved in 10 mL of purified hot water. After the crystals had completely dissolved, the solution was mixed with a gelling agent, and then the precursor solution was poured into a flat polystyrene vessel. Gelation of the mixture and subsequent crystal growth in the gel media were achieved by lowering the temperature from 60–100°C to 25°C (method 1).[19] The detailed concentration ranges to obtain the twisted and helical morphologies are described in our previous work[19] and in the figure legends.

Crystallization method 2: We also performed gelation and crystal growth simultaneously by evaporation of water from the mixture at 25°C (method 2). The 1–5 mL of the precursor solution were poured into a flat polystyrene vessel. Helical forms of $K_2Cr_2O_7$ were obtained from the follow concentration ranges; $C_{KC} = 1$–3, $C_{pv} = 0.2$, $C_{PAA} = 2.0$–4.0, $C_{ge} = 0.6$–1.0, $C_{ag} = 0.2$, and $C_{pe} = 0.2$–0.4. C_{KC}, C_{pv}, C_{PAA}, C_{ge}, C_{ag}, and C_{pe} indicate the initial concentration (g/100 g water) of $K_2Cr_2O_7$, PVA, PAA ($\bar{M}_W = 250000$; 35wt% aqueous solution), gelatin, agar, and pectin, respectively. Helical morphology of H_3BO_3 was produced from the precursor containing 1–2 g of H_3BO_3 and 0.2 g of agar per 100 g of water.

Characterization**:** Crystal morphologies were observed by using an optical microscope, a field-emission electron microscope (FESEM, Hitachi S-4700), and a field-emission transmission electron microscope (FETEM, Philips TECNAI F20). The morphologies obtained by method 2 were fundamentally the same as those by method 1. Subsequent observation of the products grown by method 2 was easily performed by using electron microscopes because the crystals were revealed with shrinkage of the matrix.

Received: September 16, 2003
Revised: November 11, 2003 [Z52891]
Published Online: January 27, 2004

Keywords: chirality · crystal growth · gels · helical structures

[1] a) D. S. Lawrence, T. Jiang, M. Levett, *Chem. Rev.* **1995**, *95*, 2229–2260; b) J.-M. Lehn, *Angew. Chem.* **1990**, *102*, 1347–1362; *Angew. Chem. Int. Ed. Engl.* **1990**, *29*, 1304–1319; c) A. H. Clark, S. B. R. Murphy, *Adv. Polym. Sci.* **1987**, *83*, 57–192.

[2] a) R. B. Prince, L. Brunsveld, E. W. Meijer, J. S. Moore, *Angew. Chem.* **2000**, *112*, 234–236; *Angew. Chem. Int. Ed.* **2000**, *39*, 228–230; b) D. A. Frankel, D. F. O'Brien, *J. Am. Chem. Soc.* **1994**, *116*, 10057–10069; c) S. Yamasaki, H. Tatumi, *Bull. Chem. Soc. Jpn.* **1994**, *67*, 906–911; d) K. Hanabusa, M. Yamada, M. Kimura, H. Shirai, *Angew. Chem.* **1996**, *108*, 2086–2088; *Angew. Chem. Int. Ed. Engl.* **1996**, *35*, 1949–1951; e) J. H. Jung, Y. Ono, K. Hanabusa, S. Shinkai, *J. Am. Chem. Soc.* **2000**, *122*, 5008–5009.

[3] a) A. L. McClellan, *J. Chem. Phys.* **1960**, *32*, 1271–1273; b) T. Tachibana, H. Kambara, *J. Am. Chem. Soc.* **1965**, *87*, 3015–3016.

[4] C. Y. Li, J. J. Ge, F. Bai, B. H. Calhoun, F. W. Harris, S. Z. D. Cheng, L. C. Chien, B. Lotz, H. D. Keith, *Macromolecules* **2001**, *34*, 3634–3641, and references therein.

[5] a) J. H. Gerorger, A. Singh, R. R. Price, J. M. Schnur, P. Yager, P. E. Schoen, *J. Am. Chem. Soc.* **1987**, *109*, 6169–6175; b) H. Ihara, M. Takafuji, C. Hirayama, D. F. O'Brien, *Langmuir* **1992**, *8*, 1548–1553; c) B. N. Thomas, C. M. Lindemann, R. C. Corcoran, C. L. Contant, J. E. Kirsch, J. P. Persichini, *J. Am. Chem. Soc.* **2002**, *124*, 1227–1233.

[6] a) W. E. Lindsell, P. N. Preston, J. M. Seddon, G. M. Rosair, A. J. Woodman, *Chem. Mater.* **2000**, *12*, 1572–1576; b) W. Yang, X. Chai, L. Chi, X. Liu, Y. Cao, R. Lu, Y. Jiang, X. Tang, H. Fuchs, T. Li, *Chem. Eur. J.* **1999**, *5*, 1144–1149.

[7] a) J. Liu, F. Zhang, T. He, *Macromol. Rapid Commun.* **2001**, *22*, 1340–1343; b) Z. Barteczak, A. S. Argon, R. E. Cohen, T. Kowalewski, *Polymer* **1999**, *40*, 2367–2380.

[8] a) R. T. K. Baer, P. S. Harris, S. Terry, *Nature* **1975**, *253*, 37–39; b) S. Yang, X. Chen, S. Motojima, *Appl. Phys. Lett.* **2002**, *81*, 3567–3569.

[9] G. W. Sears, *J. Chem. Phys.* **1959**, *31*, 53–54.

[10] B. Lotz, J. C. Wittmann, *J. Polym. Sci. Part B* **1986**, *24*, 1541 – 1558.
[11] J. M. Schultz, *Polymer* **2003**, *44*, 433 – 441, and references therein.
[12] F. Bernauer, *Gedrillte Kristalle*, Gebrüder Borntraeger, Berlin, **1929**.
[13] a) M. Li, S. Mann, *Langmuir* **2000**, *16*, 7088 – 7094; b) J. D. Hopwood, S. Mann, *Chem. Mater.* **1997**, *9*, 1819 – 1828.
[14] L. A. Gower, D. A. Tirrell, *J. Cryst. Growth* **1998**, *191*, 153 – 160.
[15] a) J. M. Garcia-Ruiz, *J. Cryst. Growth* **1985**, *73*, 251 – 262; b) T. Terada, S. Yamabi, H. Imai, *J. Cryst. Growth* **2003**, *253*, 435 – 444.
[16] J. Suda, T. Nakayama, A. Nakahara, M. Matsushita, *J. Phys. Soc. Jpn.* **1996**, *95*, 771 – 777.
[17] O. Giraldo, S. L. Brock, M. Marquez, S. L. Suib, H. Hillhouse, M. Tsapatsis, *Nature* **2000**, *405*, 38.
[18] a) S. M. Yang, I. Sokolov, N. Coombs, C. T. Kresge, G. A. Ozin, *Adv. Mater.* **1999**, *11*, 1427 – 1431; b) W. J. Kim, S. M. Yang, *Adv. Mater.* **2001**, *13*, 1191 – 1194c) A. M. Seddon, H. M. Patel, S. L. Burkett, S. Mann, *Angew. Chem.* **2002**, *114*, 3114 – 3117; *Angew. Chem. Int. Ed.* **2002**, *41*, 2988 – 2991.
[19] Y. Oaki, H. Imai, *Cryst. Growth Des.* **2003**, *3*, 711 – 716.
[20] X. Weng, C. Y. Li, S. Jin, D. Zhang, J. Z. Zhang, F. Bai, F. W. Harris, S. Z. D. Cheng, *Macromolecules* **2002**, *35*, 9678 – 9686.
[21] M. J. Buerger, *Am. Mineral.* **1945**, *30*, 469 – 482.
[22] A. M. Cody, R. D. Cody, *J. Cryst. Growth* **1995**, *151*, 369 – 374.

